Dalton Transactions

PAPER

View Article Online
View Journal

Luminescent alkynyl-gold(I) coumarin derivatives and their biological activity†

Cite this: DOI: 10.1039/c3dt52594e

Julià Arcau,[a] Vincent Andermark,[b] Elisabet Aguiló,[a,c] Albert Gandioso,[a] Artur Moro,[d] Mario Cetina,‡[c] João Carlos Lima,[d] Kari Rissanen,[c] Ingo Ott[b] and Laura Rodríguez*[a]

Received 19th September 2013,
Accepted 16th November 2013

DOI: 10.1039/c3dt52594e

www.rsc.org/dalton

The synthesis and characterization of three propynyloxycoumarins are reported in this work together with the formation of three different series of gold(I) organometallic complexes. Neutral complexes are constituted by water soluble phosphines (PTA and DAPTA) which confer water solubility to them. The X-ray crystal structure of 7-(prop-2-in-1-yloxy)-1-benzopyran-2-one and its corresponding dialkynyl complex is also shown and the formation of rectangular dimers for the gold derivative in the solid state can be observed. A detailed analysis of the absorption and emission spectra of both ligands and complexes allows us to attribute the luminescent behaviour to the coumarin organic ligand. Moreover, the presence of the gold(I) metal atom seems to be responsible for an increase of coumarin phosphorescence emission. The biological activity of the complexes showed that the anionic complexes triggered strong cytotoxic effects in two different cell lines whereas the neutral gold alkynyl complexes led to lower effects against tumor cell growth. Thioredoxin reductase (TrxR) inhibition was very strong in the case of the neutral complexes (IC_{50} values below 0.1 μM) but moderate for the anionic complexes (IC_{50} values above 0.8 μM).

Introduction

There has been increasing interest over the last 20 years in organometallic complexes containing alkynyl units because of their potential application in different fields in chemistry, such as molecular electronics, chemical sensors and materials science. In particular, gold(I) derivatives are studied mainly due to their well-known luminescent properties which are due not only to the structural characteristic of their ligands but also to the possible establishment of Au(I)···Au(I) interactions.[1–4]

More recently, the interest in these compounds from the biological point of view is increasing and the results are quite promising.[5–10] Gold derivatives have gained increasing attention due to their generally strong tumour cell growth inhibiting effects and the observation that many such compounds inhibit the enzyme thioredoxin reductase (TrxR).[11–15] TrxR is an ubiquitous flavoprotein in charge of regeneration of the functionality of small molecules (*e.g.* thioredoxin and glutathione) which are oxidized by different xenobiotics or enzymes belonging to the antioxidant network, and responsible for controlling the cellular redox homeostasis. Consequently the selective inhibition of this key enzyme represents a valuable parameter for the development of new gold-based anticancer drugs.[16]

The main goal in the development of new bioactive gold complexes is the preparation of complexes that show suitable stability under physiological conditions.[8] In fact, recent initial reports on the bioactivity of alkynyl gold complexes indicate

[a]*Departament de Química Inorgànica, Universitat de Barcelona, Barcelona, Spain. E-mail: laura.rodriguez@qi.ub.es; Fax: +34 934907725; Tel: +34 934039130*
[b]*Institute of Medicinal and Pharmaceutical Chemistry, Technische Universität Braunschweig, Beethovenstr. 55, 38106 Braunschweig, Germany*
[c]*Department of Chemistry, Nanoscience Center, University of Jyväskylä, P.O. Box 35, 40014 Jyväskylä, Finland*
[d]*REQUIMTE, Departamento de Química, CQFB, Universidade Nova de Lisboa, Monte de Caparica, Portugal*

† Electronic supplementary information (ESI) available: ^{1}H-NMR spectrum of compound **2** in $CDCl_3$ (Fig. S1); ^{13}C-NMR spectrum of compound **2** in $CDCl_3$ (Fig. S2); ESI-MS(+) spectrum of compound **2** (Fig. S3); molecular structure for **2** (Fig. S4); crystal packing along the *b* axis (left) and view of the six hydrogen bonds that connect the molecules of **2** in the crystal (right). Reference molecule is shown in black color (Fig. S5); crystal packing of **2** along the *a* axis (Fig. S6); ^{1}H-NMR spectrum of **2a** in $CDCl_3$ (Fig. S7); ^{13}C-NMR spectrum of **2a** in $CDCl_3$ (Fig. S8); ESI-MS(+) spectrum of compound **2a** (Fig. S9); crystal packing of **2a** along the *b* axis. Insert: π···π interaction between two anionic units of **2a** (Fig. S10); ^{1}H-NMR spectrum of **2b** in $CDCl_3$ (Fig. S11); ^{13}C-NMR spectrum of **2b** in $CDCl_3$ (Fig. S12); ^{1}H-NMR spectrum of **2c** in $CDCl_3$ (Fig. S13); ^{13}C-NMR spectrum of **2c** in $CDCl_3$ (Fig. S14); absorption spectra of **1–3** in methanol at *ca.* 1×10^{-5} M concentration (Fig. S15); emission spectra of **1–3**. λ_{exc} = 294 nm for **1** and 320 nm for **2** and **3** (Fig. S16); emission spectra of **1–3** recorded at 77 K. λ_{exc} = 294 nm for **1** and 320 nm for **2** and **3** (Fig. S17); emission spectra of **1–3a** recorded at 77 K. λ_{exc} = 294 nm for **1a** and 320 nm for **2a** and **3a** (Fig. S18); emission spectra of **1–3b/c** recorded at 77 K. λ_{exc} = 294 nm for **1b/c** and 320 nm for **2b/c** and **3b/c** (Fig. S19). X-ray crystallographic data for **2** and **2a** in CIF format (CCDC 955660 and 955661) (Table S1); selected bond lengths [Å] and angles [°] of **2** (Table S2); selected bond lengths [Å] and angles [°] for **2a** (Table S3). CCDC 955660 and 955661. For ESI and crystallographic data in CIF or other electronic format see DOI: 10.1039/c3dt52594e

‡ Present address: Department of Applied Chemistry, Faculty of Textile Technology, University of Zagreb, Prilaz baruna Filipovića 28a, HR-10000 Zagreb, Croatia.

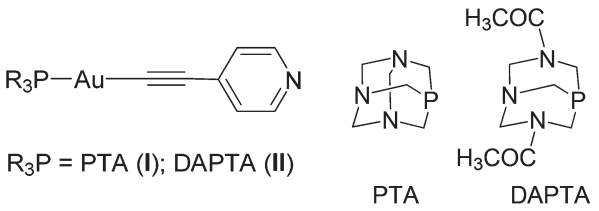

Chart 1

that this type of organometallic complex offers opportunities for the development of new chemotherapeutics against cancer and infectious diseases.[6] Despite their potential, only very few studies on the biological potential of alkynyl gold complexes have been reported so far.[5,7–9,17]

Very recent studies developed by us have shown that a series of [Au_2(diphosphine)(4-ethynylpyridyl)$_2$] complexes present some activity against TrxR but their low solubility in water and their weak luminescence were limiting factors for biological applications.[17] In order to improve the observed biological activity, in this work we have analyzed the effect of replacing the previous organic diphosphanes with the water-soluble phosphanes PTA (1,3,5-triaza-7-phosphaadamantane) and DAPTA (3,7-diacetyl-1,3,7-triaza-5-phosphabicyclo[3.3.1]-nonane) (Chart 1). This change should confer moderate to high water solubility on these complexes that could facilitate drug administration and transport in the body. Moreover, the compounds have shown gel formation in water[18,19] and this fact could be also considered as a positive point to improve the drug transfer through the cell membrane.

On the other hand, the 4-ethynylpyridyl organic ligand has been modified by a coumarine functionalized by a propynyloxy group at 4- or 7-position (Chart 2) in order to obtain neutral and anionic gold(I) alkynyl–coumarin complexes. Coumarine derivatives exist in a wide variety of different structures due to the different substitution possibilities within their basic structure that contains a benzene ring fused to an α-pyrone. These ligands are chosen because of their antiinflammatory,[20] antioxidant,[21] antithrombotic,[22] antiviral,[23] antimicrobial[24] and anticarcinogenic[25] properties. The possible modifications on their chemical structure might be able to modulate their corresponding biological activity.[26,27] Moreover, coumarins exhibit in general high emission quantum yields and due to their excellent optical properties can find application in organic light-emitting diodes (OLED),[28] non-linear optical chromophores,[29] and fluorescent sensors and labels including physiological measurement, among others.[30]

Experimental section

General procedures

All manipulations were performed under prepurified N_2 using standard Schlenk techniques. All solvents were distilled from appropriate drying agents. Commercial reagents propargyl bromide, 4-hydroxy-1-benzopyran-2-one, 7-hydroxy-1-benzopyran-2-one, 4-methyl-7-hydroxy-1-benzopyran-2-one, 1,3,5-triaza-7-phosphaadamantane (PTA) and 3,7-diacetyl-1,3,7-triaza-5-phosphabicyclo[3.3.1]nonane (DAPTA) were used as received from Sigma Aldrich Company. Literature methods were used to prepare [PPh_4][$Au(acac)_2$],[31] [Au(C≡C–C_5H_4N)-(PTA)],[18] and [Au(C≡C–C_5H_4N)(DAPTA)].[19]

Physical measurements

Infrared spectra were recorded on a FT-IR 520 Nicolet Spectrophotometer. ^{1}H NMR (δ(TMS) = 0.0 ppm) and ^{31}P{^{1}H}-NMR (δ (85% H_3PO_4) = 0.0 ppm) spectra were obtained on a Varian Unity 400 and a Varian Inova 300. Elemental analyses of C, H, N and S were carried out at the Serveis Científico-Tècnics in Barcelona. ES(+) mass spectra were recorded on a Fisons VG Quatro spectrometer. Absorption spectra were recorded on a Varian Cary 100 Bio UV-spectrophotometer and emission spectra on Horiba-Jobin-Yvon SPEX Fluorolog 3.22 and Nanolog spectrofluorimeters. Emission quantum yields were measured by employing 7-methoxy-4-methylcoumarin as a reference (ϕ_F = 0.124, 25 °C, methanol) for the excitation of the samples at 294 nm (**1**, **1a–c**) and 320 nm (**2**, **3**, **2a–c**, **3a–c**). For fluorescence decays, the samples were excited at 280 nm using a nanoled (IBH). The electronic start pulses were shaped

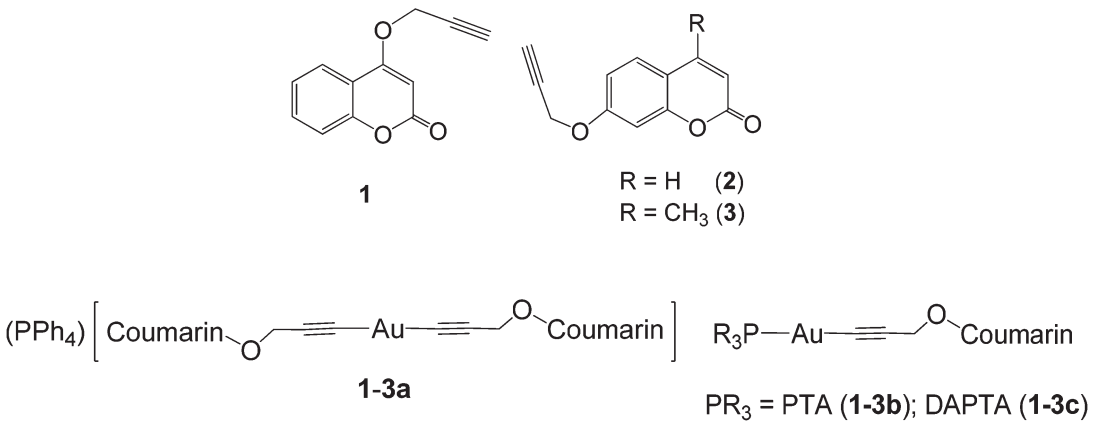

Chart 2

in a constant fraction discriminator (Canberra 2126) and directed to a time to amplitude converter (TAC, Canberra 2145). The emission wavelength was selected by a monochromator (Oriel 77250), imaged in a fast photomultiplier (9814B Electron Tubes Inc.), and the PM signal was shaped as before and delayed before entering the TAC as stop pulses. The analogue TAC signals were digitized (ADC, ND582) and stored in a multichannel analyzer installed in a PC (1024 channels, 38.1 ps per ch). The analysis of the decays is carried out with the method of modulating functions extended by global analysis as implemented by Striker.[32]

Synthesis of 4-(prop-2-in-1-yloxy)-1-benzopyran-2-one (1). This complex has been synthesized based on a method reported in the literature[33] with small modifications.

Solid 4-hydroxy-1-benzopyran-2-one (1.2 g, 7.42 mmol) and K_2CO_3 (1.28 g, 9.29 mmol) were dissolved in deoxygenated acetone (120 ml). After 5 min of stirring, propargyl bromide (830 μl, 9.31 mmol) was added dropwise and the solution of the reaction was stirred for 18 h at 50 °C. The solution of the reaction was concentrated to dryness and extracted with ethyl acetate–H_2O and recrystallized with ethyl acetate–hexane to give a pale pink solid in 50% yield (460 mg, 2.30 mmol). ^{1}H-NMR ($CDCl_3$, ppm): δ 7.84 (dd, 1H, J = 8.0 Hz, J = 1.6 Hz, C–CH–C*H*–), 7.57 (ddd, 1H, J = 8.7 Hz, 7.3 Hz, 1.6 Hz, O–C–CH–C*H*–), 7.33 (d, 1H, J = 8.4 Hz, O–C–C*H*), 7.31–7.27 (m, 1H, C–C–CH–C*H*–), 5.84 (s, 1H, O–CO–C*H*), 4.87 (d, 2H, J = 2.4 Hz, CH_2), 2.67 (t, J = 2.4 Hz, 1H, C≡C*H*). ^{13}C{^{1}H} NMR (100 MHz, $CDCl_3$): δ = 164.4 (s, C10); 162.6 (s, C8); 153.5 (s, C2); 132.7 (s, C6); 124.2 (s, C5); 123.2 (s, C4); 117.0 (s, C1); 115.5 (s, C3); 91.9 (s, C9); 78.1 (s, CH$_2$–*C*≡C); 75.9 (s, CH$_2$–C≡*C*); 57.0 (s, C14). IR (KBr, cm^{-1}): 3278 (≡C–H), 2125 (C≡C), 1716 (C═O). ES-MS (+) m/z: 201.06 ([M + H]$^+$, calc: 201.05). Anal. Calc. C, 72.00, H, 4.03%; found C, 72.05, H, 4.06%.

Synthesis of 7-(prop-2-in-1-yloxy)-1-benzopyran-2-one (2). This complex has been synthesized based on a method reported in the literature[34] with small modifications.

Solid 7-hydroxy-1-benzopyran-2-one (1.2 g, 7.42 mmol) and K_2CO_3 (1.28 g, 9.29 mmol) were dissolved in deoxygenated acetone (120 ml). After 5 min of stirring, propargyl bromide (830 μl, 9.31 mmol) was added dropwise and the solution of the reaction was stirred for 36 h at 50 °C. The solution of the reaction was concentrated to dryness, extracted with ethyl acetate–H_2O and purified by silica chromatography using dichloromethane–ethyl acetate, 9 : 1, as an eluent to obtain a white solid in 73% yield (1.1 g, 5.49 mmol). ^{1}H-NMR ($CDCl_3$, ppm): δ 7.65 (d, 1H, J = 9.5 Hz, O–CO–C*H*), 7.41 (d, 1H, J = 8.5 Hz, O–CO–CH–CH–C–C*H*), 6.95 (d, 1H, J = 2.4 Hz, O–C–C*H*), 6.92 (dd, 1H, J = 8.5 Hz, 2.5 Hz, CH$_2$–O–C–C*H*), 6.29 (d, 1H, J = 9.5 Hz, O–CO–CH–C*H*), 4.77 (d, 2H, J = 2.4 Hz, CH_2), 2.58 (t, J = 2.4 Hz, 1H, C≡C*H*). ^{13}C{^{1}H} NMR (100 MHz, $CDCl_3$): δ = 161.1 (s, C8); 160.7 (s, C6); 155.8 (s, C2); 143.4 (s, C10); 129.0 (s, C4); 113.8 (s, C3); 113.3 (s, C9); 113.2 (s, C5); 102.3 (s, C1); 77.4 (s, CH$_2$–*C*≡C); 76.7 (s, CH$_2$–C≡*C*); 56.4 (s, C14). IR (KBr, cm^{-1}): 3275 (≡C–H), 2122 (C≡C), 1717 (C═O). ES-MS (+) m/z: 201.05 ([M + H]$^+$, calc: 201.05). Anal. Calc. C, 72.00, H, 4.03%; found C, 72.04, H, 4.05%.

Synthesis of 4-methyl-7-(prop-2-in-1-yloxy)-1-benzopyran-2-one (3). Details of the synthesis of **2** were also applied to the preparation of this compound using 4-methyl-7-(prop-2-in-1-yloxy)-1-benzopyran-2-one instead of 7-(prop-2-in-1-yloxy)-1-benzopyran-2-one to obtain a white solid in 77% yield (1.13 g, 5.27 mmol). ^{1}H-NMR ($CDCl_3$, ppm): δ 7.53 (dd, 1H, J = 8.2 Hz, 1.0 Hz, O–C–C*H*–CH), 6.97–6.91 (m, 2H, O–C–CH–C*H* + O–C–C*H*–C), 6.16 (q, 1H, J = 1.2 Hz, CO–C*H*–C), 4.76 (d, 2H, J = 2.4 Hz, CH_2), 2.57 (t, J = 2.4 Hz, 1H, C≡C*H*), 2.41 (d, 3H, J = 1.2 Hz, CH_3). ^{13}C{^{1}H} NMR (100 MHz, $CDCl_3$): δ = 161.3 (s, C8); 160.5 (s, C6); 155.2 (s, C10); 152.2 (s, C2); 125.8 (s, C4); 114.4 (s, C3); 112.9 (s, C9); 112.6 (s, C5); 102.3 (s, C1); 77.6 (s, CH$_2$–*C*≡C); 76.6 (s, CH$_2$–C≡*C*); 56.3 (s, C14); 18.8 (s, C16). IR (KBr, cm^{-1}): 3303 (≡C–H), 2122 (C≡C), 1721 (C═O). ES-MS (+) m/z: 215.07 ([M + H]$^+$, calc: 215.07), 237.05 ([M + Na]$^+$, calc: 237.05), 429.14 ([2M + H]$^+$, calc: 429.15), 451.12 ([2M + Na]$^+$, calc: 451.13). Anal. Calc. C, 72.89, H, 4.71%; found C, 72.92, H, 4.73%.

Synthesis of [PPh$_4$][Au{4-(prop-2-in-1-yloxy)-1-benzopyran-2-one}$_2$] (1a). Solid 4-(prop-2-in-1-yloxy)-1-benzopyran-2-one (96 mg, 0.48 mmol) was added to a dichloromethane solution (15 ml) of [PPh$_4$][Au(acac)$_2$] (158 mg, 0.22 mmol). The reaction was stirred at room temperature for 45 min protected from light with aluminium foil and then filtered with Celite. The resulting solution was concentrated to 2 ml and diethylether (10 ml) was added. A brown solid was obtained in 31% yield (62 mg, 0.07 mmol). ^{1}H-NMR ($CDCl_3$, ppm): δ 7.84–7.65 (m, 22H, P*Ph*$_4$ + O–C–C–C*H*), 7.50–7.46 (m, 2H, O–C–CH–C*H*), 7.22–7.18 (m, 4H, O–C–C*H* + C–C–CH–C*H*), 5.69 (s, 2H, CO–C*H*–C), 4.84 (s, 4H, CH_2). ^{13}C{^{1}H} NMR (100 MHz, $CDCl_3$): δ = 165.1 (s, C10); 162.8 (s, C8); 153.2 (s, C2); 135.6–116.1 (m, Ph + PPh$_4^+$); 92.5 (s, C9); 91.1 (s, CH$_2$–C≡*C*); 77.2 (s, CH$_2$–*C*≡C); 59.6 (s, C14). IR (KBr): 2158 cm^{-1} ν(C≡C). IR (KBr, cm^{-1}): 2120 (C≡C), 1719 (C═O). ES-MS (–) m/z: 595.06 ([M]$^-$, calc: 595.05). Anal. Calc. C, 61.68, H, 3.67%; found C, 61.70, H, 3.69%.

Synthesis of [PPh$_4$][Au{7-(prop-2-in-1-yloxy)-1-benzopyran-2-one}$_2$] (2a). Details of the synthesis of **1a** were also applied to the preparation of this compound using 7-(prop-2-in-1-yloxy)-1-benzopyran-2-one instead of 4-(prop-2-in-1-yloxy)-1-benzopyran-2-one. A pale yellow solid was obtained in 48% yield (132 mg, 0.14 mmol). ^{1}H NMR ($CDCl_3$, ppm): δ 7.86–7.63 (m, 20H, P*Ph*$_4$), 7.60 (d, 2H, J = 9.2 Hz, O–CO–C*H*), 7.33 (m, 2H, O–C–CH–C*H*), 6.94 (m, 2H, O–C–C*H*–C), 6.73 (s, 2H, O–C–C*H*–CH), 6.17 (m, 2H, CO–CH–C*H*), 4.74 (s, 4H, CH_2). ^{13}C{^{1}H} NMR (100 MHz, $CDCl_3$): δ = 161.9 (s, C8); 161.3 (s, C6); 155.5 (s, C2); 143.6 (s, C10); 135.7–102.6 (m, C9 + Ph + PPh$_4^+$); 94.2 (s, CH$_2$–C≡*C*); 77.2 (s, CH$_2$–*C*≡C); 58.6 (s, C14). IR (KBr, cm^{-1}): 2120 (C≡C), 1727 (C═O). ES-MS (–) m/z: 595.05 ([M]$^-$, calc: 595.05). Anal. Calc. C, 61.68, H, 3.67%; found C, 61.71, H, 3.68%.

Synthesis of [PPh$_4$][Au{4-methyl-7-(prop-2-in-1-yloxy)-1-benzopyran-2-one}$_2$] (3a). Details of the synthesis of **1a** were also applied to the preparation of this compound using 4-methyl-7-(prop-2-in-1-yloxy)-1-benzopyran-2-one instead of 4-(prop-2-in-1-yloxy)-1-benzopyran-2-one. A pale yellow solid was obtained in 38% yield (96 mg, 0.10 mmol). ^{1}H NMR ($CDCl_3$, ppm):

δ 7.85–7.64 (m, 20H, P*Ph*$_4$), 7.43 (d, 2H, J = 8.9 Hz, O–C–CH–C*H*), 6.99 (dd, 2H, J = 8.8 Hz, 2.3 Hz, O–C–C*H*–CH), 6.70 (d, 2H, J = 2.3 Hz, O–C–C*H*–C), 6.04 (s, 2H, CO–C*H*–C), 4.74 (s, 4H, CH_2), 2.36 (s, 6H, CH_3). ^{13}C{^{1}H} NMR (100 MHz, $CDCl_3$): δ = 161.7 (s, C8); 161.4 (s, C6); 154.9 (s, C10); 152.7 (s, C2); 135.6–102.7 (m, Ph + PPh_4^+ + C9); 94.23 (s, CH_2–C≡*C*); 77.0 (s, CH_2–*C*≡C); 58.6 (s, C14); 18.7 (s, C16, Me). IR (KBr, cm^{-1}): 2121 (C≡C), 1722 (C═O). ES-MS (–) m/z: 623.08 ([M]$^-$, calc: 623.08). Anal. Calc. C, 62.38, H, 3.98%; found C, 62.41, H, 4.00%.

Synthesis of [Au{4-(prop-2-in-1-yloxy)-1-benzopyran-2-one}-(PTA)] (1b). Solid KOH (8 mg, 0.15 mmol) was added to a solution of 4-(prop-2-in-1-yloxy)-1-benzopyran-2-one (25 mg, 0.14 mmol) in methanol (5 ml). After 5 min of stirring a dichloromethane solution (5 ml) of [AuCl(PTA)] (41 mg, 0.10 mmol) was added and the solution was maintained at room temperature protected from light with aluminium foil. After 2 hours of stirring, the solution was concentrated to *ca.* 2 ml and hexane (5 ml) was added to precipitate a pale yellow solid which was filtered and obtained in 65% yield (41 mg, 0.07 mmol). ^{1}H-NMR ($CDCl_3$, ppm): 7.85 (dd, J = 9 Hz, 3 Hz, 1H, C–C–C*H*), 7.52 (td, J = 9 Hz, J = 3 Hz, 1H, O–C–CH–C*H*), 7.28 (m, 2H, O–C–C*H* + C–C–CH–C*H*), 5.95 (s, 1H, CO–C*H*), 4.95 (s, 2H, CH_2), 4.60–4.46 (AB q, J = 13 Hz, 6H, N–CH_2–N), 4.29 (s, 6H, N–CH_2–P). ^{31}P{^{1}H}-NMR ($CDCl_3$, ppm): −51.0. ^{13}C{^{1}H} NMR (100 MHz, $CDCl_3$): δ = 170.1 (s, C═O); 164.4 (s, C10); 163.0 (s, C8); 143.4 (s, C2); 129.7 (s, C6); 128.6 (s, C5); 115.9 (s, C4); 114.0 (s, C1); 113.2 (s, C3); 102.7 (s, C9); 77.4 (s, CH_2–C≡*C*); 76.7 (s, CH_2–*C*≡C); 73.4 (d, J = 7 Hz, PCH_2N); 56.5 (s, C14), 52.5 (s, NCH_2N). IR (KBr, cm^{-1}): 2138(CC), 1729, 1618 (C═O). ES-MS (+) m/z: 554.08 ([M + H$^+$]$^+$, calc: 554.08). Anal. Calc. C, 39.07, H, 3.46, N, 7.59%; found C, 39.10, H, 3.48, N, 7.61%.

Synthesis of [Au{7-(prop-2-in-1-yloxy)-1-benzopyran-2-one}-(PTA)] (2b). Details of the synthesis of **1b** were also applied to the preparation of this compound using 7-(prop-2-in-1-yloxy)-1-benzopyran-2-one instead of 4-(prop-2-in-1-yloxy)-1-benzopyran-2-one. A pale yellow solid was obtained in 37% yield (25 mg, 0.05 mmol). ^{1}H-NMR ($CDCl_3$, ppm): 7.64 (d, J = 9 Hz, 1H, CO–CH–C*H*), 7.36 (d, J = 9 Hz, 1H, O–C–CH–C*H*), 7.05 (s, 1H, O–C–C*H*–C), 6.91 (dd, J = 9 Hz, 3 Hz, 1H, O–C–C*H*–CH), 6.26 (d, J = 9 Hz, 1H, O–CO–C*H*), 4.84 (s, 2H, CH_2), 4.60–4.46 (AB q, J = 13 Hz, 6H, N–CH_2–N), 4.24 (s, 6H, N–CH_2–P). ^{31}P{^{1}H}-NMR ($CDCl_3$, ppm): −51.1. ^{13}C{^{1}H} NMR (100 MHz, $CDCl_3$): δ = 170.2 (s, C═O); 164.6 (s, C10); 163.1 (s, C8); 143.6 (s, C2); 129.9 (s, C6); 128.7 (s, C5); 115.5 (s, C4); 113.7 (s, C1); 113.2 (s, C3); 102.5 (s, C9); 77.4 (s, CH_2–C≡*C*); 76.7 (s, CH_2–*C*≡C); 73.5 (d, J = 7 Hz, PCH_2N); 57.5 (s, C14), 52.6 (s, NCH_2N). IR (KBr, cm^{-1}): 2139 (C≡C), 1725, 1624 (C═O). ES-MS (+) m/z: 554.08 ([M + H$^+$]$^+$, calc: 554.08). Anal. Calc. C, 39.07, H, 3.46, N, 7.59%; found C, 39.09, H, 3.47, N, 7.57%.

Synthesis of [Au{4-methyl-7-(prop-2-in-1-yloxy)-1-benzopyran-2-one}(PTA)] (3b). Details of the synthesis of **1b** were also applied to the preparation of this compound using 4-methyl-7-(prop-2-in-1-yloxy)-1-benzopyran-2-one instead of 4-(prop-2-in-1-yloxy)-1-benzopyran-2-one. A pale yellow solid was obtained in 49% yield (34 mg, 0.06 mmol). ^{1}H-NMR ($CDCl_3$, ppm): 7.49 (d, J = 9 Hz, 1H, O–C–CH–C*H*), 7.05 (s, 1H, O–C–C*H*–C), 6.94 (dd, J = 9 Hz, 3 Hz, 1H, O–C–C*H*–CH), 6.13 (s, 1H, CO–C*H*–C), 4.83 (s, 2H, CH_2), 4.60–4.46 (AB q, J = 13 Hz, 6H, N–CH_2–N), 4.19 (s, 6H, N–CH_2–P), 2.39 (s, 3H, CH_3). ^{31}P{^{1}H}-NMR ($CDCl_3$, ppm): −51.1. ^{13}C{^{1}H} NMR (100 MHz, $CDCl_3$): δ = 170.2 (s, C═O); 164.5 (s, C10); 163.1 (s, C8); 144.0 (s, C2); 129.9 (s, C6); 128.9 (s, C5); 116.0 (s, C4); 113.8 (s, C1); 113.4 (s, C3); 102.7 (s, C9); 77.3 (s, CH_2–C≡*C*); 76.6 (s, CH_2–*C*≡C); 73.4 (d, J = 7 Hz, PCH_2N); 57.4 (s, C14), 52.8 (s, NCH_2N). IR (KBr, cm^{-1}): 2124 (C≡C), 1710, 1613 (C═O). ES-MS (+) m/z: 568.1 ([M + H$^+$]$^+$, calc: 568.1). Anal. Calc. C, 40.22, H, 3.73, N, 7.41%; found C, 40.24, H, 3.74, N, 7.39%.

Synthesis of [Au{4-(prop-2-in-1-yloxy)-1-benzopyran-2-one}-(DAPTA)] (1c). Details of the synthesis of **1b** were also applied to the preparation of this compound but using DAPTA instead of PTA. A pale yellow solid was obtained in 37% yield (29 mg, 0.05 mmol). ^{1}H-NMR ($CDCl_3$, ppm): 7.85 (dd, J = 9 Hz, 3 Hz, 1H, C–C–C*H*), 7.52 (td, J = 9 Hz, 3 Hz, 1H, O–C–CH–C*H*), 7.28 (m, 2H, O–C–C*H* + C–C–CH–C*H*), 5.99 (s, 1H, CO–C*H*), 5.80 (d, J = 12 Hz, 1H, N–CH_2–N), 5.70 (dd, J = 15 Hz, 9 Hz, 1H, N–CH_2–P), 4.97 (d, J = 12 Hz, 1H, N–CH_2–N), 4.97 (s, 2H, CH_2), 4.88 (m, 1H, N–CH_2–P), 4.68 (d, J = 15 Hz, 1H, N–CH_2–N), 4.14 (d, J = 15 Hz, 1H, N–CH_2–P), 4.07 (d, J = 15 Hz, 1H, N–CH_2–N), 3.84(s, 2H, N–CH_2–P), 3.50 (d, J = 15 Hz, 1H, N–CH_2–P), 1.59 (s, 6H, N–CO–CH_3). ^{31}P{^{1}H}-NMR ($CDCl_3$, ppm): −22.6. ^{13}C{^{1}H} NMR (100 MHz, $CDCl_3$): δ = 170.2 (s, C═O); 170.0 (s, C═O); 164.8 (s, C10); 163.3 (s, C8); 153.6 (s, C2); 132.4 (s, C6); 124.0 (s, C5); 123.4 (s, C4); 116.8 (s, C1); 116.1 (s, C3); 92.1 (s, C9); 77.4 (s, CH_2–C≡*C*); 76.6 (s, CH_2–*C*≡C); 67.5 (s, NCH_2N); 62.1 (s, NCH_2N); 58.4 (s, C14); 49.7 (d, J = 31 Hz, PCH_2N); 45.0 (d, J = 29 Hz, PCH_2N); 39.5 (d, J = 30 Hz, PCH_2N); 21.7 (s, DAPTA CH_3); 21.4 (s, DAPTA CH_3). IR (KBr, cm^{-1}): 2130 (C≡C), 1717, 1622 (C═O). ES-MS (+) m/z: 626.1 ([M + H$^+$]$^+$, calc: 626.1). Anal. Calc. C, 40.33, H, 3.71, N, 6.72%; found C, 40.36, H, 3.73, N, 6.74%.

Synthesis of [Au{7-(prop-2-in-1-yloxy)-1-benzopyran-2-one}-(DAPTA)] (2c). Details of the synthesis of **2b** were also applied to the preparation of this compound using DAPTA instead of PTA. A pale yellow solid was obtained in 35% yield (28 mg, 0.04 mmol). ^{1}H-NMR ($CDCl_3$, ppm): 7.61 (d, J = 12 Hz, 1H, CO–CH–C*H*), 7.33 (d, J = 9 Hz, 1H, O–C–CH–C*H*), 7.02 (s, 1H, O–C–C*H*–C), 6.87 (dd, J = 9 Hz, 3 Hz, 1H, O–C–C*H*–CH), 6.22 (d, J = 9 Hz, 1H, O–CO–C*H*), 5.80 (d, J = 15 Hz, 1H, N–CH_2–N), 5.64 (dd, J = 15 Hz, 9 Hz, 1H, N–CH_2–P), 4.92 (d, J = 12 Hz, 1H, N–CH_2–N), 4.85 (s, 2H, CH_2), 4.61 (d, J = 15 Hz, 1H, N–CH_2–N), 4.59 (m, 1H, N–CH_2–P), 4.08 (d, J = 15 Hz, 1H, N–CH_2–P), 4.01 (d, J = 15 Hz, 1H, N–CH_2–N), 3.78 (s, 2H, N–CH_2–P), 3.48 (d, J = 15 Hz, 1H, N–CH_2–P), 1.59 (s, 6H, N–CO–CH_3). ^{31}P{^{1}H}-NMR ($CDCl_3$, ppm): −22.6. ^{13}C{^{1}H} NMR (100 MHz, $CDCl_3$): δ = 170.2 (s, C═O); 170.0 (s, C═O); 161.9 (s, C8); 161.3 (s, C6); 155.6 (s, C10); 152.9 (s, C2); 125.8 (s, C4); 113.9 (s, C3); 113.3 (s, C9); 112.1 (s, C5); 103.1 (s, C1); 77.4 (s, CH_2–C≡*C*); 76.6 (s, CH_2–*C*≡C); 67.3 (s, NCH_2N); 62.1 (s, NCH_2N); 57.9 (s, C14); 49.3 (d, J = 30 Hz, PCH_2N); 44.9 (d, J = 29 Hz, PCH_2N); 39.5 (d, J = 30 Hz, PCH_2N); 21.8 (s, DAPTA CH_3); 21.5 (s, DAPTA CH_3). IR (KBr, cm^{-1}): 2130 (C≡C), 1717, 1622 (C═O). ES-MS (+) m/z: 626.1 ([M + H$^+$]$^+$, calc: 626.1). Anal. Calc. C, 40.33, H, 3.71, N, 6.72%; found C, 40.35, H, 3.74, N, 6.69%.

Synthesis of [Au{4-methyl-7-(prop-2-in-1-yloxy)-1-benzopyran-2-one}(DAPTA)] (3c). Details of the synthesis of **3b** were also applied to the preparation of this compound but using DAPTA instead of PTA. A pale yellow solid was obtained in 33% yield (26 mg, 0.04 mmol). ^{1}H-NMR ($CDCl_3$, ppm): 7.50 (d, J = 9 Hz, 1H, O–C–CH–C*H*), 7.07 (s, 1H, O–C–C*H*–C), 6.93 (dd, J = 9, 3 Hz, 1H, O–C–C*H*–CH), 6.13 (s, 1H, O–CO–C*H*), 5.80 (d, J = 15 Hz, 1H, N–CH_2–N), 5.64 (dd, J = 15 Hz, 9 Hz, 1H, N–CH_2–P), 4.96 (d, J = 12 Hz, 1H, N–CH_2–N), 4.89 (s, 2H, CH_2), 4.65 (d, J = 15 Hz, 1H, N–CH_2–N), 4.56 (m, 1H, N–CH_2–P), 4.12 (d, J = 15 Hz, 1H, N–CH_2–P), 4.06 (d, J = 15 Hz, 1H, N–CH_2–N), 3.87 (s, 2H, N–CH_2–P), 3.52 (d, J = 15 Hz, 1H, N–CH_2–P), 1.59 (s, 6H, N–CO–CH_3). ^{31}P{^{1}H}-NMR ($CDCl_3$, ppm): −22.6. ^{13}C{^{1}H} NMR (100 MHz, $CDCl_3$): δ = 170.2 (s, C=O); 169.8 (s, C=O); 161.4 (s, C8); 161.1 (s, C6); 155.2 (s, C10); 152.8 (s, C2); 125.7 (s, C4); 114.0 (s, C3); 113.3 (s, C9); 112.2 (s, C5); 102.2 (s, C1); 77.4 (s, CH_2–C≡*C*); 76.6 (s, CH_2–*C*≡C); 67.4 (s, NCH_2N); 62.1 (s, NCH_2N); 57.9 (s, C14); 49.3 (d, J = 26 Hz, PCH_2N); 45.0 (d, J = 27 Hz, PCH_2N); 39.6 (d, J = 28 Hz, PCH_2N); 21.8 (s, DAPTA CH_3); 21.5 (s, DAPTA CH_3); 18.8 (s, C16 (CH_3)). IR (KBr, cm^{-1}): 2115(C≡C), 1712, 1613 (C=O). ES-MS (+) m/z: 640.1 ([M + H$^+$]$^+$, calc: 640.1). Anal. Calc. C, 41.33, H, 3.94, N, 6.57%; found C, 41.35, H, 3.95, N, 6.55%.

TrxR inhibition assay. To determine the inhibition of TrxR an established microplate reader based assay was performed with minor modifications.[35] For this purpose commercially available recombinant rat liver TrxR 1 (from IMCO Corporation Ltd AB) was used and diluted with distilled water to achieve a concentration of 0.05 U ml^{-1}. The compounds were freshly dissolved as stock solutions in DMF. To each 25 μL aliquot of the enzyme solution, 25 μL of potassium phosphate buffer pH 7.0 containing the compounds in graded concentrations or the vehicle (DMF) without compounds (control probe) were added and the resulting solutions (final concentration of DMF: max. 0.5% V/V) were incubated with moderate shaking for 75 minutes at 37 °C in a 96 well plate. To each well 225 μL of a reaction mixture (1000 μL of the reaction mixture consisted of 500 μL potassium phosphate buffer pH 7.0, 80 μL 100 mM EDTA solution pH 7.5, 20 μL BSA solution 0.2%, 100 μL of 20 mM NADPH solution and 300 μL of distilled water) were added and the reaction was started by addition of 25 μL of a 20 mM ethanolic dithio-bis-2-nitrobenzoic acid (DTNB) solution. After proper mixing, the formation of 5-thio-2-nitrobenzoic acid (5-TNB) was monitored with a microplate reader (Perkin Elmer Victor X4) at 405 nm in 35 s intervals for 350 s. For each tested compound the non-interference with the assay components was confirmed by a negative control experiment using an enzyme free solution. The IC_{50} values were calculated as the concentration of the compound on decreasing the enzymatic activity of the untreated control by 50% and are given as the means and error of 2–3 independent experiments.

Cell culture and antiproliferative effects. MDA MB-231 breast adenocarcinoma and HT-29 colon carcinoma were maintained in DMEM high glucose (PAA) supplemented with 50 mg L^{-1} gentamycin and 10% (V/V) fetal calf serum (FCS) at 37 °C under a 5% CO_2 atmosphere and passaged every seven days. Antiproliferative effects were determined essentially as described in a recent publication.[35] A volume of 100 μL of a 38 000 cells per ml (HT-29) or 40 000 cells per ml (MDA-MB-231) suspension were seeded into 96-well plates and incubated for 48 hours at 37 °C and 5% CO_2. After the incubation period the cells in one plate were fixed by addition of 100 μL of a 10% glutaraldehyde solution and the plate was stored at 4 °C (t_0 plate). Stock solutions of the compounds were freshly prepared in DMF and diluted with cell culture medium to the final concentrations (0.1% v/v DMF). In the remaining plates the medium was replaced by different concentrations of the compound in cell culture medium (6 wells for each concentration). Twelve wells of each plate were treated with a solution of 0.1% DMF in cell culture medium (untreated control). Then the plates were incubated for 72 h (HT-29) or 96 h (MDA-MB-231) at 5% CO_2 and 37 °C. The medium was removed and the cells were treated with 100 μL of a 10% glutaraldehyde solution. Afterwards the cells of all plates were washed with 180 μL PBS and stained with 100 μL of a 0.02% crystal violet solution for 30 minutes. The crystal violet solution was removed and the plates were washed with water and dried. A volume of 180 μL of 70% ethanol was added to each well and after 3–4 h of gentle shaking the absorbance was measured at 595 nm in a microplate reader (Victor X4, PerkinElmer). The mean absorbance value of the t_0 plate was subtracted from the absorbance values of all other absorbance values. The IC_{50}-values were calculated as the concentrations reducing the cellular proliferation in comparison with the untreated control by 50% and are given as the means and errors of 2–4 independent experiments.

X-ray crystal structure determination. Data for **2** were collected at 170 K on an Agilent SuperNova diffractometer with an Atlas detector using mirror-monochromated Mo-Kα radiation (λ = 0.71073 Å). Data for **2a** were collected at 123 K on an Agilent SuperNova Dual diffractometer with an Atlas detector using mirror-monochromatized Cu-Kα radiation (λ = 1.54184 Å). The *CRYSALISPRO*[36] program was used for the data collection and processing of both crystals. The intensities were corrected for absorption using the multi-scan absorption correction method.[36] The structure of **2** was solved using direct methods with *SIR-2002*,[37] while the structure of **2a** was solved by charge flipping with *SUPERFLIP*.[38] Both structures were refined by full-matrix least-squares calculations based on F^2 using *SHELXL-2013*[39] integrated in the *WINGX*[40] program package. Hydrogen atoms were included in calculated positions as riding atoms, with *SHELXL-2013*[39] defaults. X-ray crystallographic data for **2** and **2a** are given in Table S1 (see ESI†).

CCDC-955660 (for **2**) and 955661 (for **2a**) contain the supplementary crystallographic data for this paper.

Results and discussion

Synthesis and characterization

Synthesis of the propynyloxycoumarin ligands. The organic ligands have been prepared by slight modifications of a

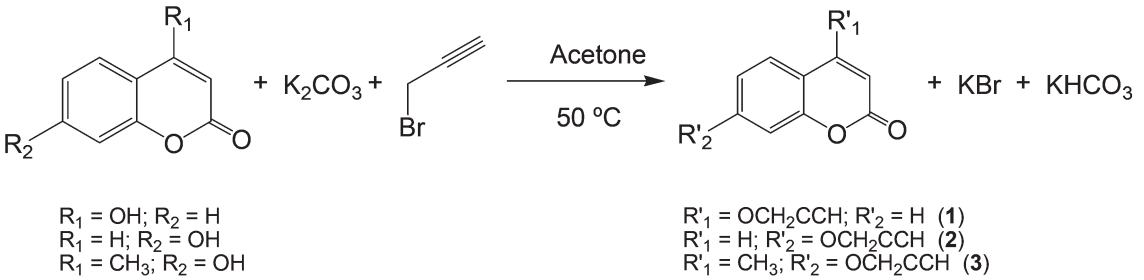

Scheme 1 Synthesis of propynyloxycoumarins **1–3**.

method previously reported in the literature (Scheme 1).[33,34] The reaction of the hydroxycoumarin (in 4 or 7 position) with propargyl bromide in acetone at 50 °C for 18–36 h and in the presence of K_2CO_3 gives the corresponding propynyloxycoumarin in pure form after recrystallization in ethyl acetate–hexane (**1**) or column chromatography purification (**2**, **3**) in high yields (*ca.* 75%).

The compounds have been characterized by ^1H and ^{13}C NMR, IR, mass spectrometry and elemental analyses (Fig. S1–S3†) showing the presence of the typical vibrations of both carbonyl and terminal alkynyl groups in the same molecule.

We have successfully grown single crystals of compound **2** suitable for X-ray diffraction experiment. The molecular structure is presented in Fig. S4† and the selected distances and angles are given in Table S2.†

As expected, the aromatic rings are within the same plane with a very small distortion angle of 1.6° between both aromatic ring planes. The C3–C4 distance is identical to that obtained for compound **3**[41] and is indicative of a double bond between these atoms. These values are very close to those reported for a similar compound containing an ethoxy group instead of a propynyloxy (1.351, 1.432 and 1.432 Å respectively).[42]

Nevertheless, there are clear differences in the crystal packing of **2** and **3**.[41] This is due to the angle between the plane calculated through O3–C11–C12–C13 atoms and the benzene ring (C5–C10), the angle being 72.5° in **2** while it is close to 0° for **3**.[41]

As can be observed in Fig. S5,† molecules are displayed in groups of two which are stacked in columns. Each pair of molecules is found to be in antiparallel disposition with distances between both aromatic centroids (one from each molecule) of 3.962(1) Å, interplanar stacking spacings of 3.3446(7) Å and ring offset of *ca.* 2.12 Å which is in agreement with the presence of π–π stacking interactions (Fig. S5 left, and S6†).

It can be also seen in Fig. S5† (right) that each molecule establishes six hydrogen bonds with their neighbours stabilizing the observed three dimensional disposition of the ligand in the solid state. The planar structure of **3**[41] may preclude this large number of weak interactions between molecules since the propynyloxy group is in the same plane as the coumarin.

Synthesis of gold(I) complexes. Two different kinds of organometallic gold(I) complexes have been synthesized: (i) anionic dialkynyl complexes **(1–3)a;** and (ii) neutral alkynyl phosphine complexes (series **(1–3)b**, containing the phosphine PTA, and **(1–3)c**, containing the phosphine DAPTA).

The anionic complexes have been synthesized by the reaction of the $(PPh_4)[Au(acac)_2]$ with the corresponding alkynyl ligand (**1–3**) in dichloromethane according to Scheme 2.

Complexes were characterized by different spectroscopical techniques (IR, ^1H and ^{13}C NMR), mass spectrometry and elemental analyses. The disappearance of the terminal alkynyl protons is shown by IR and ^1H-NMR being clear evidence of the formation of the complexes. Moreover, the methylene protons close to the alkynyl group are displayed as a singlet instead of a doublet (observed in the free organic ligand) upon coordination to the metal atom (Fig. S7†).

ESI-MS(−) spectrometry shows the molecular peak for all complexes (*e.g.* Fig. S9†).

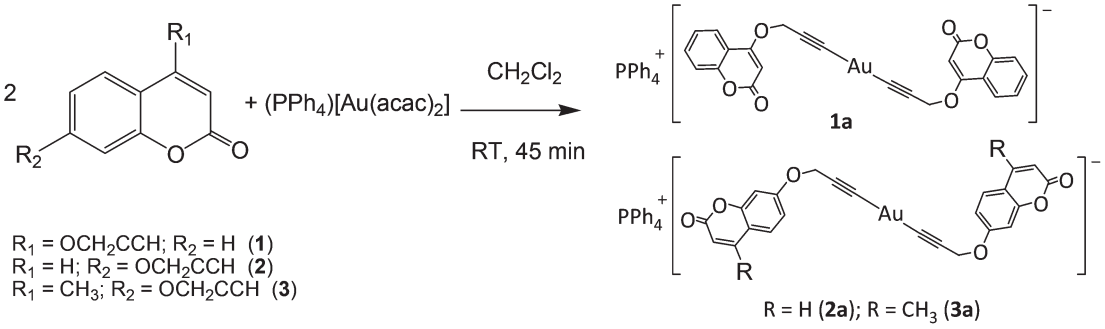

Scheme 2 Synthesis of dialkynyl gold(I) complexes **1–3a**.

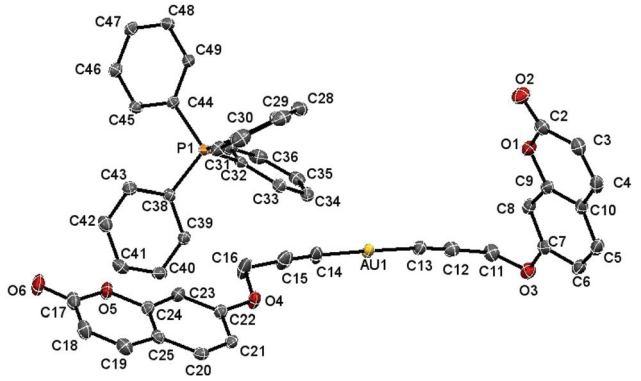

Fig. 1 Molecular structure of **2a**. Hydrogen atoms have been omitted for clarity.

Single crystals suitable for X-ray diffraction analysis for **2a** were obtained from acetone. The molecular structure of **2a** is presented in Fig. 1 and the selected bond distances and angles are summarized in Table 1.

The ligands are not symmetrically positioned around the Au(I) as can be observed from Fig. 4. One of them is pointing out of the plane constituted by the Au atom and the two C≡C moieties (C12/C13/Au1/C14/C15) and aromatic ring C5–C10, with an angle of 82.1°, slightly higher than that observed for **2** (72.5°). The other organic ligand coordinated to the metal atom is almost in the C≡C–Au–C≡C plane (4.3° deviation).

Table 1 Selected bond lengths [Å] and angles [°] for **2a**

Distance	(Å)	Angle	(°)
Au1–C13	2.004(3)	C13–Au1–C14	178.71(11)
Au1–C14	2.007(3)	C11–C12–C13	176.9(3)
C3–C4	1.344(4)	C14–C15–C16	177.5(4)
C11–C12	1.470(4)		
C12–C13	1.188(4)		
C14–C15	1.178(5)		
C15–C16	1.464(4)		
C18–C19	1.338(5)		

The C13–Au1–C14 angle is nearly linear (Table 2), and very similar to that observed for other gold(I) dialkynyl complexes previously reported in the literature.[43–45] Methylene groups are also almost in the same plane as the alkynyl moieties with angles of 176.9(3) and 177.5(4)° for C11–C12–C13 and C14–C15–C16, respectively, and in accord with that of **2** (177.6(2)°, Table 1). The hydrogen bonds in **2a** (Fig. 2) are established between the carbonyl oxygen atoms and one of the hydrogen atoms of the coumarin group (dashed lines in Fig. 2) giving rise to the formation of a dimer and a supramolecular rectangle-like structure.

The intermolecular Au···Au distance in the H-bonded dimer is 9.68 Å (Fig. 2). The PPh_4^+ cations are located outside the anionic dimers with a P···P distance of 11.02 Å and interact with the dimer through four H-bonds.

The π–π stacking interactions are also observed between the parallel-stacked aromatic rings (α = 0°) of the adjacent molecules, the distance between the C5–C10 ring centroids being

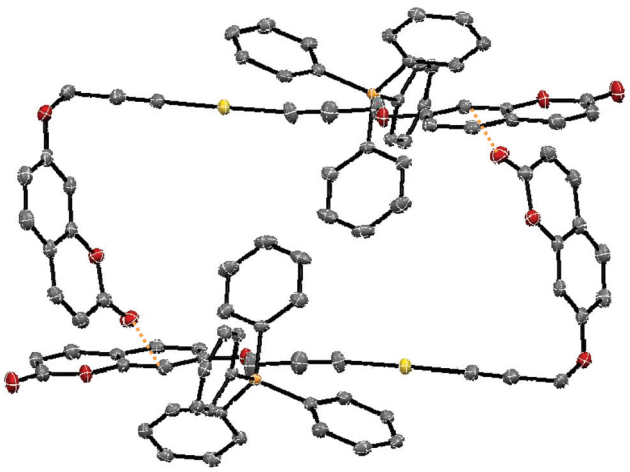

Fig. 2 Part of the crystal structure of **2a**, showing the hydrogen-bonding dimer of the anions. Hydrogen bonds are shown by a dashed orange line.

Table 2 Absorption and emission data for the organic ligands and gold(I) derivatives in methanol. λ_{exc} = 294 nm (**1**, **1a–c**) and 320 nm for the other compounds

	Absorption λ_{max} (nm) (10^{-3} ε (M^{-1} cm^{-1}))	Emission (λ_{max} (nm))	τ (ns)	Φ_{Fluor}	I_{Phosp}/I_{Fluor} at 77 K
1	264 (8.8), 275 (8.2), 302 (5.1)	350	[a]	0.001	4.35
2	295sh (9.0), 319 (13.6)	384	[b]	0.021	0.09
3	287sh (8.8), 318 (16.0)	370	0.08	0.055	0.22
1a	267 (18.9), 276 (18.6), 302 (11.6)	364	0.14	0.005	2.91
2a	269 (6.6), 275 (7.5), 322 (12.4)	384	0.41	0.060	0.12
3a	270 (8.4), 276 (9.5), 321 (21.6)	384	0.42	0.123	0.33
1b	263 (11.0), 275 (8.8), 302 (5.0)	359	0.08	0.002	[c]
2b	295sh (8.7), 320 (10.5)	381	0.16	0.058	1.46
3b	289sh (6.9), 320 (13.4)	374	0.40	0.134	2.73
1c	265 (7.8), 276 (7.4), 303 (4.6)	351	0.12	0.001	[c]
2c	296sh (8.6), 323 (14.2)	382	0.12	0.049	1.24
3c	289sh (8.1), 321 (16.7)	379	0.40	0.130	1.93

[a] Fluorescence signal was too low to record time correlated spectra. [b] Below 38.1 ps (resolution limit). [c] Only phosphorescence emission is observed.

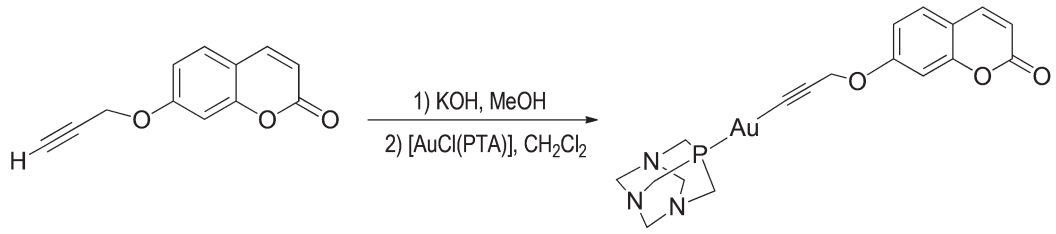

Scheme 3 Synthesis of alkynyl phosphine gold(I) complexes **1–3b**. Similar reactions were carried out for the synthesis of **1–3c** using [AuCl(DAPTA)] instead of [AuCl(PTA)].

3.646(2) Å, interplanar spacings of 3.531(1) Å and offset of *ca.* 0.91 Å (Fig. S10†).

The synthesis of the neutral alkynyl phosphine gold(I) complexes **1–3b** and **1–3c** has been carried out by deprotonation of the terminal alkynyl proton of **1–3** with a KOH methanol solution and addition of a stoichiometric quantity of [AuCl(PTA)] complex in dichloromethane (**1–3b**) (Scheme 3) or [AuCl(DAPTA)] (**1–3c**).

Characterization of the complexes by ^{1}H and ^{31}P-NMR and IR spectroscopy and ESI(+) mass spectrometry indicates the formation of the complexes. As reported for **1–3a**, IR and ^{1}H-NMR show that the disappearance of the terminal alkynyl proton is a crucial signal of the successful preparation of the complexes. The corresponding protons of the phosphine follow the typical patterns of PTA (Fig. S11†) and DAPTA (Fig. S13†). ^{31}P-NMR shows a downfield shift of about 50 ppm upon coordination of the phosphine to the gold(I) metal atom, as observed for other similar compounds.[5,18,19,46]

Molecular peaks have been obtained by ESI(+) mass spectrometry for all the monoprotonated species.

Photophysical characterization

The photophysical properties of Au(I) alkynyl complexes are now a research field in gold(I) organometallic chemistry since this property can be used for a wide range of different applications.[2] For this, absorption and emission spectra were recorded for the complexes and respective organic ligands in methanol at *ca.* 10^{-5} M concentration. The results are summarized in Table 2.

As can be seen in Fig. 3 and S15,† the absorption spectra of the organic ligands and respective gold(I) derivatives present the same profiles that depend on the substituents on the coumarin ligand, indicating that the recorded electronic spectra correspond to the coumarin ligand in all cases. It is well known that the photophysical properties of the coumarin derivatives can be tuned with small changes in the substituents and their position.[47] Thus, ligands **2** and **3** (with the substituent at the 7 position) display a similar profile with a red shifted band and higher extinction coefficients in comparison with that recorded for **1**.

Two different bands can be distinguished: (i) in the case of compounds **2** and **3** a single band between 300 and 320 nm; (ii) in the case of compound **1** and the corresponding derivatives, two bands are observed, one at *ca.* 300 nm and a second vibronically structured transition around 270 nm. In any case, bands observed are assigned to the π–π* transition of the coumarin units.[48–53]

Emission spectra recorded upon excitation of all the samples at the lowest energy band display a broad emission band centred at 350–380 nm due to the coumarin emission[48–50] (Fig. 4 and S16†). Excitation spectra collected at the emission maxima reproduce absorption of the coumarin units, which is indicative of the origin of these emission bands.

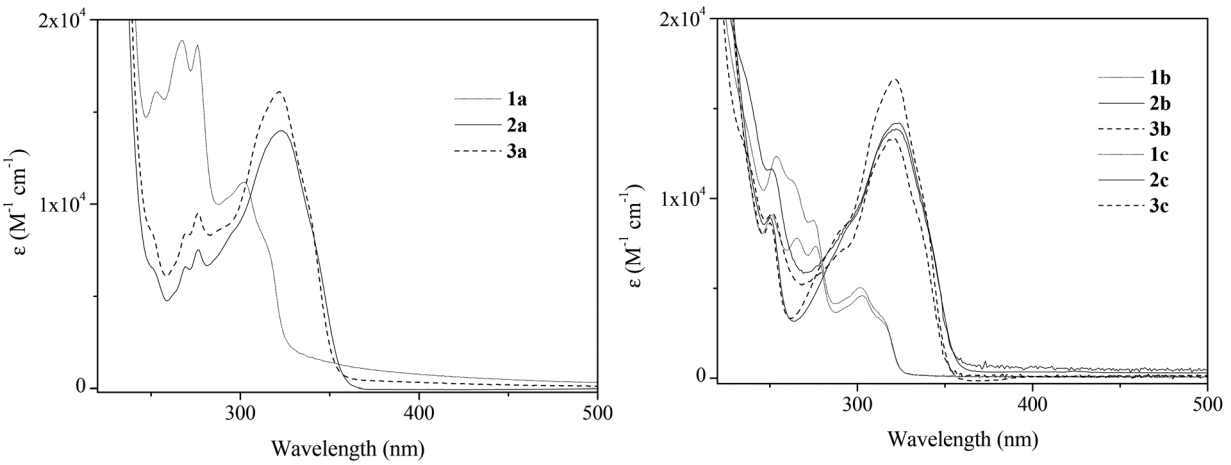

Fig. 3 Absorption spectra of complexes **1–3a** (left) and **1–3b** and **1–3c** (right).

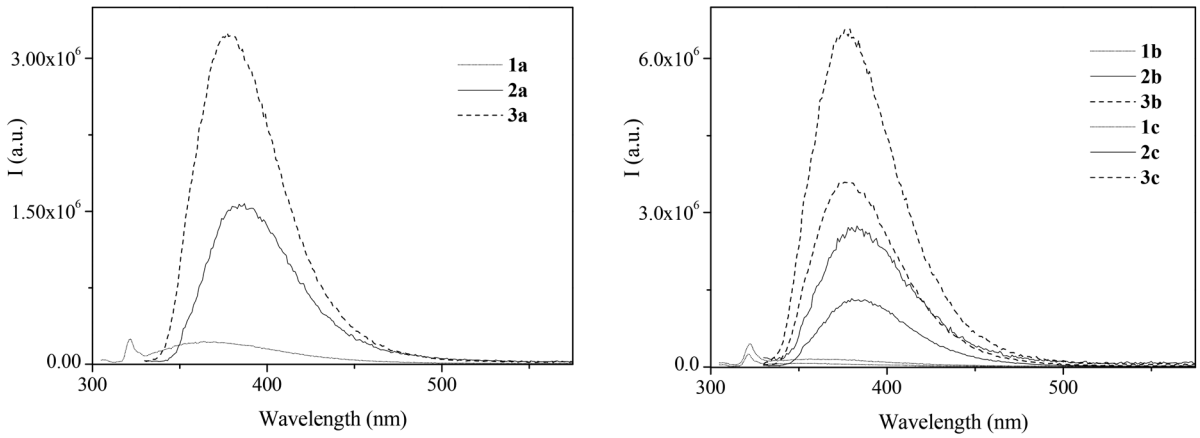

Fig. 4 Emission spectra of complexes **1–3a** (left) and **1–3b** and **1–3c** (right). λ_{exc} = 294 nm for **1** and derivatives and 320 nm for **2**, **3** and the corresponding derivatives.

The effect of the substituents on the coumarin group is also clearly evidenced in their luminescence properties since compound **1** (substituted at 4-position by the propynyloxy group) and their gold(I) complexes (**1a**, **1b** and **1c**) display a blue shifted band and very weak emission with respect to **2** and **3** derivatives. This is clearly reflected in the emission quantum yields that are at least one order of magnitude lower for the former group (see Table 2). Interestingly, the presence of a methyl group in compound **3** and the corresponding complexes affects both the recorded quantum yields and the luminescence lifetimes, with a significant increase being recorded for both parameters.

Luminescence spectra carried out at 77 K show the phosphorescence of coumarin in all cases (Fig. S17–S19). In fact, although **1** derivatives show the lowest fluorescence emission among all the complexes, coumarin triplet emission is the most important for these compounds as can be seen in the I_{Phosp}/I_{Fluor} calculated ratio (Table 2) being the triplet, the only luminescence originating from complexes **1b** and **1c** at 77 K.

Table 3 IC_{50} values (μM) for cytotoxicity in HT-29 and MDA-MB-231 cells and TrxR inhibition; n.d., not determined. Mean values ± errors of 2–4 independent experiments

	HT-29	MDA-MB-231	TrxR
1	>100	>100	n.d.
2	>100	>100	n.d.
3	>100	>100	n.d.
PTA	>100	>100	n.d.
DAPTA	>100	>100	n.d.
PPh_4Cl	1.38 ± 0.85	1.61 ± 0.93	>10
$PPh_4[AuCl_2]$	1.69 ± 1.24	1.90 ± 1.20	0.052 ± 0.003
1a	1.84 ± 0.82	3.43 ± 1.61	0.858 ± 0.106
2a	2.13 ± 1.66	2.21 ± 1.17	>1
3a	3.14 ± 0.86	4.08 ± 1.92	1.031 ± 0.053
1b	20.34 ± 0.03	13.10 ± 0.62	0.093 ± 0.003
2b	27.28 ± 7.03	15.76 ± 2.81	0.044 ± 0.018
3b	41.40 ± 1.67	13.32 ± 3.60	0.049 ± 0.016
1c	74.30 ± 3.70	44.96 ± 8.82	0.065 ± 0.007
2c	65.86 ± 4.11	63.99 ± 5.33	0.041 ± 0.010
3c	76.25 ± 6.17	67.42 ± 20.67	0.063 ± 0.033
I	56.09 ± 3.05	52.32 ± 4.76	0.085 ± 0.005
II	74.78 ± 9.34	34.07 ± 3.51	0.054 ± 0.019

Biological evaluation

The biological evaluation focused on determining the effects against tumor cell growth in HT-29 colon carcinoma and MDA-MB-231 breast cancer cells as well as inhibition of the activity of the enzyme TrxR, which represents a well established molecular target of gold species. The results are summarized in Table 3.

The anionic complexes **1a–3a** triggered strong cytotoxic effects in both cell lines with IC_{50} values in the low micromolar range whereas the coumarin ligands **1–3** were inactive. However, with these examples the cytotoxicity may be mostly related to the counterion PPh_4^+ that also showed high activity in the form of its chloride salt or as $PPh_4[AuCl_2]$. The neutral gold alkynyl complexes **1–3b/c** and **I**, **II** led to lower effects against tumor cell growth. Since the coumarin derivatives **1–3** as well as PTA and DAPTA and ethynylpyridyne[17] were not cytotoxic (no IC_{50} values below 100 μM), the effects are in this case clearly related to the presence of the gold atoms in the complexes.

Interestingly, TrxR inhibition was very strong in the case of the neutral complexes **1–3b/c**, **I** and **II** (IC_{50} values below 0.1 μM) but moderate for the anionic complexes **1a–3a** (IC_{50} values above 0.8 μM). In fact, the activities of **1–3b/c**, **I** and **II** were comparable to that of $PPh_4[AuCl_2]$, in which gold(I) is not stably coordinated and readily available to interact with thiols/selenols as present in TrxR. Moreover, their activity was also similar to that of some other recently studied complexes of the alkynyl gold(I) triphenylphosphane type.[8]

Conclusions

The synthesis of new propynyloxycoumarin gold(I) derivatives containing an alkynyl unit or water soluble phosphines at the second coordinative position of the metal atom has given rise to interesting photophysical properties that depend on the organic ligand.

X-ray crystal structures of 7-(prop-2-in-1-yloxy)-1-benzopyran-2-one and its corresponding dialkynyl complex show the establishment of weak interactions in both cases and the formation of rectangular dimers for the gold derivative.

The luminescence of all complexes is due to the organic ligands and it has been observed that the presence of the gold(I) metal atom plays an important role in the phosphorescence of coumarins. Moreover, luminescence is almost quenched for those derivatives containing a propynyloxy group at the 4-coumarin position.

The anionic complexes triggered strong cytotoxic effects in HT-29 colon carcinoma and MDA-MB-231 breast cancer cell lines with IC_{50} values in the low micromolar range whereas all the organic precursors were inactive. However, the strong activity of the anionic complexes may be driven by their PPh_4^+ counterions.

The neutral gold alkynyl complexes led to lower effects against tumor cell growth with a clear preference for the PTA over the DAPTA phosphine ligand and the effects are clearly related to the presence of the gold atoms in the complexes.

TrxR inhibition was very strong for the neutral complexes but moderate for the anionic ones.

Acknowledgements

The support and sponsorship provided by COST Actions CM1005 and CM1105 are acknowledged. Authors are also grateful to the Ministerio de Ciencia e Innovación of Spain (project CTQ2012–31335), Fundação para a Ciência e Tecnologia of Portugal (PTDC/QUI-QUI/112597/2009; PEst-C/EQB/LA0006/2011), Deutsche Forschungsgemeinschaft (DFG, grant OT 338/7–1) and Academy of Finland (KR, grant no. 265328 and 263256). A.M. thanks FCT for a post-doctoral grant (SFRH/BPD/69210/2010).

References

1 *Comprenhensive Supramolecular Chemistry*, ed. J. L. Atwood, J. E. D. Davies, D. D. MacNicol, F. Vögtle and K. S. Suslick, Pergamon Press, Oxford, 1996.
2 J. C. Lima and L. Rodríguez, *Chem. Soc. Rev.*, 2011, **40**, 5442–5446.
3 L. Rodríguez, M. Ferrer, R. Crehuet, J. Anglada and J. C. Lima, *Inorg. Chem.*, 2012, **51**, 7636–7641.
4 R. Gavara, L. Rodríguez and J. C. Lima, *submitted*.
5 E. Vergara, E. Cerrada, A. Casini, O. Zava, M. Laguna and P. J. Dyson, *Organometallics*, 2010, **29**, 2596–2603.
6 J. C. Lima and L. Rodríguez, *Anticancer Agents Med. Chem.*, 2011, **11**, 921–928.
7 E. Schuh, S. M. Valiahdi, M. A. Jakupec, B. K. Keppler, P. Chiba and F. Mohr, *Dalton Trans.*, 2009, 10841–10845.
8 A. Meyer, C. P. Bagowski, M. Kokoschka, M. Stefanopoulou, H. Alborzinia, S. Can, D. H. Vlecken, W. S. Sheldrick, S. Wölfl and I. Ott, *Angew. Chem., Int. Ed.*, 2012, **51**, 8895–8899.
9 C.-H. Chui, R.-M. Wong, R. Gambari, G. Y.-M. Cheng, M. C.-W. Yuen, K.-W. Chan, S.-W. Tong, F.-Y. Lau, P. B.-S. Lai, K.-H. Lam, C.-L. Ho, C.-W. Kan, K. S.-Y. Leung and W.-Y. Wong, *Bioorg. Med. Chem.*, 2009, **17**, 7872–7877.
10 C. Wetzel, P. C. Kunz, M. U. Kassack, A. Hamacher, P. Böhler, W. Watjen, I. Ott, R. Rubbiani and B. Spinglere, *Dalton Trans.*, 2011, **40**, 9212–9220.
11 M. J. McKeage, L. Maharaj and S. J. Berners-Price, *Coord. Chem. Rev.*, 2002, **232**, 127–135.
12 A. Bindoli, M. P. Rigobello, G. Scutarib, C. Gabbiani, A. Casini and L. Messori, *Coord. Chem. Rev.*, 2009, **253**, 1692–1707.
13 P. J. Barnard and S. J. Berners-Price, *Coord. Chem. Rev.*, 2007, **251**, 1889–1902.
14 V. Gandin, A. P. Fernandes, M. P. Rigobello, B. Dani, F. Sorrentino, F. Tisato, M. Bjornstedt, A. Bindoli, A. Sturaro, R. Rella and C. Marzano, *Biochem. Pharmacol.*, 2012, **79**, 90–101.
15 C. Gabbiani and L. Messori, *Anticancer Agents Med. Chem.*, 2011, **11**, 929–939.
16 R. Rubbiani, E. Schuh, A. Meyer, J. Lemke, J. Wimberg, N. Metzler-Nolte, F. Meyer, F. Mohr and I. Ott, *Med. Chem. Commun.*, 2013, **4**, 942–948.
17 A. Meyer, A. Gutiérrez, I. Ott and L. Rodríguez, *Inorg. Chim. Acta*, 2013, **398**, 72–76.
18 R. Gavara, J. Llorca, J. C. Lima and L. Rodríguez, *Chem. Commun.*, 2013, **49**, 72–74.
19 E. Aguiló, R. Gavara, J. C. Lima, J. Llorca and L. Rodríguez, *J. Mater. Chem. C*, 2013, **1**, 5538–5547.
20 M. Ghate, D. Manohar, V. Kulkarni, R. Shobha and S. Y. Kattimani, *Eur. J. Med. Chem.*, 2003, **38**, 297–302.
21 V. D. Kancheva, P. V. Boranova, J. T. Nechev and I. I. Manolov, *Biochimie*, 2010, **92**, 1138–1146.
22 J. R. S. Hoult and M. Payá, *Gen. Pharm.: Vascul. Syst.*, 1996, **27**, 713–726.
23 J. R. Hwu, R. Singha, S. C. Hong, Y. H. Chang, A. R. Das, I. Vliegen, E. De Clercq and J. Neyts, *Antiviral Res.*, 2008, **77**, 157–162.
24 T. Smyth, V. N. Ramachandran and W. F. Smyth, *Int. J. Antimicrob. Agents*, 2009, **33**, 421–426.
25 M. Prince, Y. Li, A. Childers, K. Itoh, M. Yamamoto and H. E. Kleiner, *Toxicol. Lett.*, 2009, **185**, 180–186.
26 R. O'Kennedy and R. D. Thornes, *Coumarins: biology, applications and mode of action*, Johan Wiley&Sons Ltd., England, 1997, pp. 1–336.
27 G. Magdalena and B. Elzbieta, *Coord. Chem. Rev.*, 2009, **253**, 2588–2598.
28 C. H. Chang, H. C. Cheng, Y. J. Lu, K. C. Tien, H. W. Lin, C. L. Lin, C. J. Yang and C. C. Wu, *Org. Electron.*, 2010, **11**, 247–254.
29 C. R. Moylan, *J. Phys. Chem.*, 1994, **98**, 13513–13516.
30 H. S. Jung, P. S. Kwon, J. W. Lee, J. I. Kim, C. S. Hong, J. W. Kim, S. H. Yan, J. Y. Lee, J. H. Lee, T. Joo and J. S. Kim, *J. Am. Chem. Soc.*, 2009, **131**, 2008–2012.

31 J. Vicente and M. T. Chicote, *Inorg. Synth.*, 1998, **32**, 172–177.
32 G. Striker, V. Subramaniam, C. A. M. Seidel and A. Volkmer, *J. Phys. Chem. B*, 1999, **103**, 8612–8617.
33 Ch. Prasad Rao and G. Srimannarayana, *Synth. Commun.*, 1990, **20**, 535–540.
34 I. Kosiova and P. Kois, *Collect. Czech. Chem. Commun.*, 2007, **72**, 996–1004.
35 R. Rubbiani, S. Can, I. Kitanovic, H. Alborzinia, M. Stefanopoulou, M. Kokoschka, S. Mönchgesang, W. S. Sheldrick, S. Wölfl and I. Ott, *J. Med. Chem.*, 2011, **54**, 8646–8657.
36 *Oxford Diffraction, Xcalibur CCD System. CRYSALISPRO*, Oxford Diffraction Ltd, Abingdon, England, 2013.
37 M. C. Burla, M. Camalli, B. Carrozzini, G. L. Cascarano, C. Giacovazzo, G. Polidori and R. Spagna, *J. Appl. Crystallogr.*, 2003, **36**, 1103–1103.
38 L. Palatinus and G. Chapuis, *J. Appl. Crystallogr.*, 2007, **40**, 786–790.
39 G. M. Sheldrick, *Acta Crystallogr., Sect. A: Fundam. Crystallogr.*, 2008, **64**, 112–122.
40 L. J. Farrugia, *J. Appl. Crystallogr.*, 1999, **32**, 837–838.
41 P. Toffoli, P. Khodadad and N. Rodier, *Acta Crystallogr.*, 1985, **41**, 933–935.
42 K. Ueno, *Acta Crystallogr.*, 1985, **41**, 1786–1789.
43 M. Ferrer, L. Rodríguez, O. Rossell, F. Pina, J. C. Lima, M. Font Bardia and X. Solans, *J. Organomet. Chem.*, 2003, **678**, 82–89.
44 J. Vicente, M.-T. Chicote and M. M. Alvarez-Falcón, *Organometallics*, 2005, **24**, 5956–5963.
45 J. Vicente, M.-T. Chicote and M.-D. Abrisqueta, *Organometallics*, 1997, **16**, 5628–5636.
46 E. García-Moreno, S. Gascón, M. J. Rodriguez-Yoldi, E. Cerrada and M. Laguna, *Organometallics*, 2013, **32**, 3710–3720.
47 J. S. Seixas de Melo, R. S. Becker and A. L. Maçanita, *J. Phys. Chem.*, 1994, **98**, 6054–6058.
48 J. S. Seixas de Melo, C. Cabral, J. C. Lima and A. L. Maçanita, *J. Phys. Chem. A*, 2011, **115**, 8392–8398.
49 E. Oliveira, J. L. Capelo, J. C. Lima and C. Lodeiro, *Amino Acids*, 2012, **43**, 1779–1790.
50 J. R. Heldt, J. Heldt, M. Stoń and H. A. Diehl, *Spectrochim. Acta, Part A*, 1995, **51**, 1549–1563.
51 M. Ferrer, A. Gutiérrez, L. Rodríguez, O. Rossell, J. C. Lima, M. Font-Bardía and X. Solans, *Eur. J. Inorg. Chem.*, 2008, 2899–2909.
52 E. C. Constable, C. E. Housecroft, M. K. Kocik and J. A. Zampese, *Polyhedron*, 2011, **30**, 2704–2710.
53 J. S. Seixas de Melo and P. F. Fernandes, *J. Mol. Struct.*, 2001, **565–566**, 69–78.